PNAS RESEARCH ARTICLE | MEDICAL SCIENCES

# Senolytic and senomorphic agent procyanidin C1 alleviates structural and functional decline in the aged retina

Yidan Liu[a,1], Xiuxing Liu[a,1], Xuhao Chen[a,1], Zhenlan Yang[a,1], Jianqi Chen[a], Weining Zhu[b], Yangyang Li[a], Yuwen Wen[a], Caibin Deng[a], Chenyang Gu[a], Jianjie Lv[a], Rong Ju[a], Yehong Zhuo[a,2], and Wenru Su[a,2]

Edited by Robert F. Mullins, The University of Iowa, Iowa City, IA; received June 30, 2023; accepted March 27, 2024 by Editorial Board Member Jeremy Nathans

**Increased cellular senescence burden contributes in part to age-related organ dysfunction and pathologies. In our study, using mouse models of natural aging, we observed structural and functional decline in the aged retina, which was accompanied by the accumulation of senescent cells and senescence-associated secretory phenotype factors. We further validated the senolytic and senomorphic properties of procyanidin C1 (PCC1) both in vitro and in vivo, the long-term treatment of which ameliorated age-related retinal impairment. Through high-throughput single-cell RNA sequencing (scRNA-seq), we comprehensively characterized the retinal landscape after PCC1 administration and deciphered the molecular basis underlying the senescence burden increment and elimination. By exploring the scRNA-seq database of age-related retinal disorders, we revealed the role of cellular senescence and the therapeutic potential of PCC1 in these pathologies. Overall, these results indicate the therapeutic effects of PCC1 on the aged retina and its potential use for treating age-related retinal disorders.**

cellular senescence | senescence-associated secretory phenotype | senolytics | aging | retina

## Significance

Cellular senescence burden, accumulated during natural aging, contributes to age-related dysfunction and disorders in various tissues. In this study, we validated the senescent pattern of the aged retina, both physiologically and pathologically, with high-throughput single-cell RNA sequencing. Elevation of senescent cells and senescence-associated secretory phenotype, which led to structural and functional decline of the retina, was attenuated with the application of procyanidin C1 (PCC1), a polyphenolic component of grape seed extract flavonoids. By depicting a comprehensive retinal landscape, we demonstrated the combined effect of the senolytic and senomorphic profile of PCC1. These findings unveiled the senotherapeutic potential of PCC1, which also held great promise in treating age-related retinal diseases.

Aging affects various systems in the body, leading to chronic degenerative and age-related illnesses (1–3). The retina, an essential part of the visual system, is not spared by aging. The retina is primarily composed of delicate interconnected layers of specialized neurons. Natural aging leads to a gradual decline in both the functional and structural aspects of the retina (4). As individuals age, the accumulation of harmful stressors can result in pathological changes such as neuronal dendritic sprouting and glial cell activation (3, 5), which can ultimately lead to retinal degeneration and an increased risk of visual impairment. Age-related retinal disorders, including age-related macular degeneration (AMD), diabetic retinopathy (DR), and glaucoma, are the main pathologies encountered alongside cataract (6). Since retinal damage is associated with irreversible blindness and visual impairment, the long-term costs of treatment and eye care for the elderly can be substantial. Therefore, gaining a better understanding of natural retinal aging may help identify optimal targets for mitigating or reversing the aging process. Nevertheless, there are still knowledge gaps in this area.

Cellular senescence is a state where cells undergo permanent cell cycle arrest while remaining viable (7). It is initiated by various sources of stress and strongly linked to aging (8). Early senescent cells (SnC) exhibit increased oxidative metabolism, chromatin remodeling, and resistance to apoptosis, which may eventually lead to chronic inflammation in advanced stages of senescence (9). SnC secrete bioactive chemokines, cytokines, proteases, and growth factors, collectively known as the senescence-associated secretory phenotype (SASP). SASP factors have diverse effects, such as attracting innate immune cells, promoting chronic inflammation, inducing paracrine cellular senescence, and remodeling the tissue microenvironment. These processes can have a detrimental impact on both the SnC themselves and neighboring structures (10). When the threshold of SnC accumulation is exceeded, it ultimately leads to tissue destruction and age-related pathologies (11).

Efforts have been focused on addressing the pathogenic role of cellular senescence, aiming to make it a potentially treatable process (12). The key players involved are SnC and the senescence-associated secretory phenotype (SASP), which can be targeted through two main strategies: selective elimination of SnC using senolytics and inhibition of SASP using senomorphics (13). These approaches have been widely employed in degenerative conditions like diabetes (14), age-related cognitive impairment (1), and frailty (15) and are currently being explored in the visual system. Promising results have been observed in preclinical studies using senolytics for age-related retinal disorders (3), advancing early-phase clinical trials for conditions such as age-related macular degeneration (AMD) and diabetic macular edema (DME) (16, 17).

Author contributions: Y. Liu, X.L., Y.Z., and W.S. designed research; Y. Liu, X.L., X.C., and Z.Y. performed research; Y. Liu, X.L., X.C., Z.Y., and J.C. contributed new reagents/analytic tools; Y. Liu, X.L., Z.Y., J.C., W.Z., Y. Li, Y.W., C.D., C.G., J.L., and R.J. analyzed data; R.J. provided experimental guidance; W.S. supervised the research; and Y. Liu and X.C. wrote the paper.

The authors declare no competing interest.

This article is a PNAS Direct Submission. R.F.M. is a guest editor invited by the Editorial Board.



[1]Y. Liu, X.L., X.C., and Z.Y. contributed equally to this work.

[2]To whom correspondence may be addressed. Email: zhuoyh@mail.sysu.edu.cn or suwr3@mail.sysu.edu.cn.

This article contains supporting information online at https://www.pnas.org/lookup/suppl/doi:10.1073/pnas.2311028121/-/DCSupplemental.

Published April 24, 2024.

Nevertheless, most drugs involve only a single target, which blunts their therapeutic effects. To overcome this limitation, procyanidin C1 (PCC1), a polyphenolic compound found in grape seed extract flavonoids, shows promise. PCC1 is reportedly a neuroprotective (18) and antiproliferative agent (19), and was recently confirmed to possess both senomorphic and senolytic effects, indicating its potential to reverse retinal aging and further mitigate age-related diseases (20). However, it is still unknown whether systemic administration of PCC1 exerts a promising therapeutic effect on the aged retina. Furthermore, the therapeutic potential of selectively eliminating the cellular senescence burden in age-related retinal disorders remains to be explored.

By establishing naturally aged mouse models in the current study, we confirmed structural and functional decline in the aged retina, which was accompanied by the accumulation of SnC and SASP factors. We further validated the senolytic and senomorphic properties of PCC1 both in vitro and in vivo, which simultaneously ameliorated age-related retinal impairment. With the advent of high-throughput single-cell RNA sequencing (scRNA-seq) technology, an in-depth understanding of cellular taxonomy and intricate cellular interactions has been realized (21). In this study, we characterized a comprehensive retinal landscape after the administration of PCC1 and deciphered the molecular basis underlying senescence burden increment and elimination. We explored the scRNA-seq database for age-related retinal disorders and revealed the role of cellular senescence in these pathological conditions. Together, these results highlighted the therapeutic effect of PCC1 on the aged retina and its potential for treating age-related retinal disorders.

## Results

**The Age-Related Decline in the Retina Accompanied by Senescence Burden Accumulation.** During natural aging, cells undergo degenerative changes, resulting in a decline in the physiological functions of tissues and organs. First, to explore the effects of aging on retinal function, we recorded the electroretinogram (ERG) of young (6- to 8-wk-old) and aged (18- to 20-mo-old) mice. We found that normal ERG responses decreased with age (Fig. 1 *A* and *B* and *SI Appendix*, Fig. S1*A*), indicating a reduction in electrophysiological responses of photoreceptors and downstream neurons, which compromised visual perception in the aged retina.

Next, we investigated how aging affects retinal structure. In the young retina, rod bipolar cells (RBCs) and horizontal cells (HCs) form synapses with photoreceptors within the outer plexiform layer (OPL). However, in aged mice, the dendrites of RBCs and HCs extended from the OPL to the outer nuclear layer (ONL) (Fig. 1 *C* and *D*). Additionally, retinal glia also exhibit age-related alterations. Aging induced astrocyte and Müller glial activation, characterized by increased glial fibrillary acidic protein (GFAP) immunoreactivity, thickened cell layers, and extended cell processes (Fig. 1*E*). Moreover, the number of microglia increased (Fig. 1*F*).

The accumulation of SnC and their secretome, SASP is implicated in physical functional decline and diseases in various tissues during aging. p16+ SnC, although scarce, could be identified on the aged retina section (Fig. 1*G*). We then examined the mRNA expression, which revealed that Cdkn2a (encoding p16) and Cdkn1a (encoding p21) were increased, accompanied by the upregulation of several SASP factors including IL1B, CCL3, ERN1, CSF2, MMP3, and SERPINE1 in the aged retina (Fig. 1*H*). To further quantify cellular senescence in the retina, we performed senescence-associated β-galactosidase (SA-β-GAL) staining using flow cytometry (FC). We observed a notable increase in SA-β-GAL-positive cells in the retina of aged mice (Fig. 1*I*). Accordingly, the frequency of p16+ and p21+ cells were also increased in the aged group (Fig. 1 *J* and *K* and *SI Appendix*, Fig. S1*B*). Moreover, we examined whether there was an elevated SASP burden in the aged retina. FC analysis revealed varying degrees of upregulation in the expression of SASP cytokines IL-6, IL-1β, and TNF-α in the aged retina compared to their younger counterparts (Fig. 1 *L–N*). These cytokines play important roles in mediating inflammatory responses that contributes to senescence-associated dysfunction.

In summary, natural retinal aging was accompanied by the accumulation of SnC and SASP factors, which may lead to morphological changes and functional impairment.

**Long-Term PCC1 Treatment Relieved Functional and Structural Impairment in the Aged Retina by Both Senolytic and Senomorphic Effects.** Given the noxious role of cellular senescence in tissue degeneration, we next explored whether depleting SnC could attenuate these age-dependent alterations. We chose the novel compound PCC1 and first tested its efficacy in vitro using various retinal cell lines including 661 W (a photoreceptor cell line used as a model for retinal neurons), BV2 (a microglia cell line) and ARPE-19 (an RPE cell line). After induction of senescence (see *Materials and Methods* for details) and PCC1 treatment, we quantified the senescence burden, and the results revealed that PCC1 significantly decreased cellular senescence across all cell lineages (Fig. 2 *A–C* and *SI Appendix*, Fig. S2 *A–I*).

After confirming the senotherapeutic effect of PCC1 in vitro, we proceeded to investigate its potential in relieving senescence burden in vivo. We treated 14- to 16-mo-old mice with or without PCC1 mixed in a standard diet for 4 mo. We first used ultraperformance liquid chromatography (UPLC) to validate that PCC1 indeed entered the retina parenchyma (*SI Appendix*, Fig. S2*J*). Subsequent FC results revealed that PCC1 partially eliminated cells expressing SA-β-GAL, p16, and p21 in the total retina cell population compared with the control group (Fig. 2 *D–F*), suggesting the depletion of retinal SnC in vivo. In addition, the levels of the SASP cytokines IL-6, IL-1β, and TNF-α were decreased by PCC1 treatment (Fig. 2 *G–I*). RT-qRCR results further confirmed the significant reduction of senescence markers and SASP-associated signatures upon PCC1 treatment (*SI Appendix*, Fig. S2*K*).

We further examined whether a decrease in cellular senescence could translate to the rejuvenation of age-related retinal dysfunction. To assess this, we performed ERG and IF staining on both aged and PCC1-treated retina. The ERG recordings showed increased amplitudes of the scotopic a- and b-waves and photopic b-wave (Fig. 2 *J* and *K* and *SI Appendix*, Fig. S2*L*), indicating that impaired visual perception was restored by PCC1 treatment. Moreover, we evaluated the effects of PCC1 on synaptic aging and glial activation in the retina. PCC1 treatment ameliorated the aberrantly elongated processes of RBCs and HCs in aged mice compared to the control group (Fig. 2 *L* and *M*). In addition, PCC1 therapy reduced GFAP immunoreactivity of macroglia (Fig. 2*N*) and the number of microglia in aged mice (Fig. 2*O*).

In summary, by reducing the senescence burden, PCC1 treatment could reverse age-related degenerative structural remodeling and functional impairment in the aged retina.

**The Seotherapeutic Effects of PCC1 Treatment on the Aged Retina Evaluated by Single-Cell Analysis.** Unbiased high-throughput single-cell RNA sequencing (scRNA-seq) is a cutting-edge tool for dissecting tissue heterogeneity and uncovering molecular mechanisms. To elucidate the molecular dynamics underlying the antiaging effects of PCC1, we conducted scRNA-seq analysis on

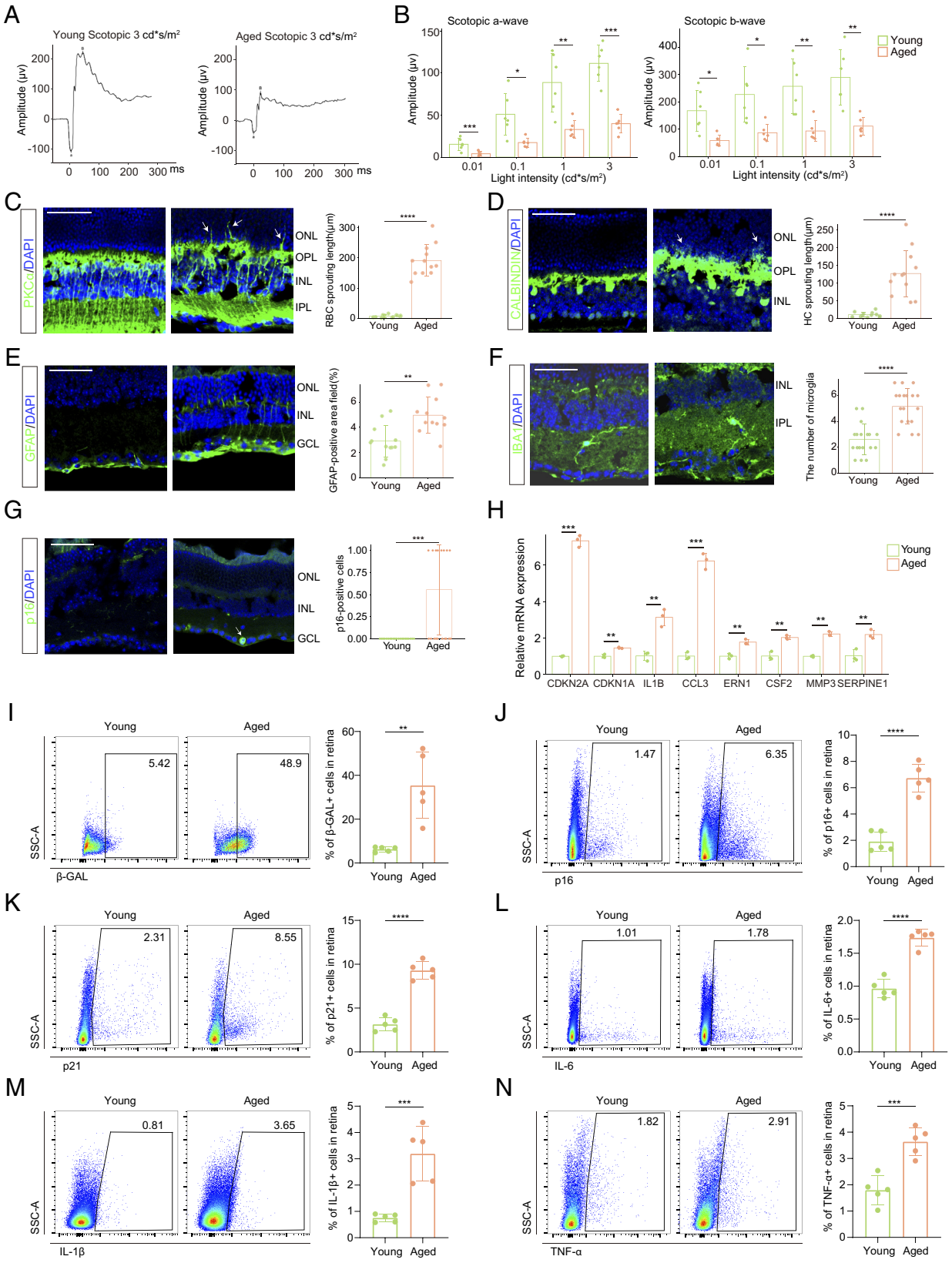


**Fig. 1.** The age-related decline in the retina accompanied by senescence burden accumulation. (*A*) Representative scotopic ERG of young and aged mice at a light density of 3 cd*s/m$^2$. (*B*) Bar charts showing the quantification of scotopic ERG amplitudes (n = 6/group). (*C–G*) Representative confocal images of retinal frozen sections of young (*Left*) and aged (*Middle*) mice and bar charts of quantification (*Right*, n = 6/group). Frozen sections are labeled with PKCα (*C*), Calbindin (*D*), GFAP (*E*), IBA1 (*F*), and p16 (*G*). Arrows indicate the abnormal sprouting dendrites of RBCs (*C*) and HCs (*D*) which extend beyond OPL into the ONL. The arrow in (*G*) indicates the p16+ cell in the retina. (Scale bar, 50 μm.) (*H*) The mRNA levels of several SASP-related genes were detected by RT-qPCR between young and old groups (n = 3/group). (*I–N*) The FC histograms (*Left*) and column charts (*Right*) showing the level of β-GAL (*I*), p16 (*J*), p21 (*K*), IL-6 (*L*), IL-1β (*M*), and TNF-α (*N*) in retinal cells between young and aged groups (n = 5/group). Data are shown as mean ± SD. *P* values were analyzed using unpaired two-tailed Student's *t* test (*B–E* and *H–N*) or two-tailed Mann–Whitney *U* test (*F* and *G*); **P* < 0.05, ***P* < 0.01, ****P* < 0.001, and *****P* < 0.0001.

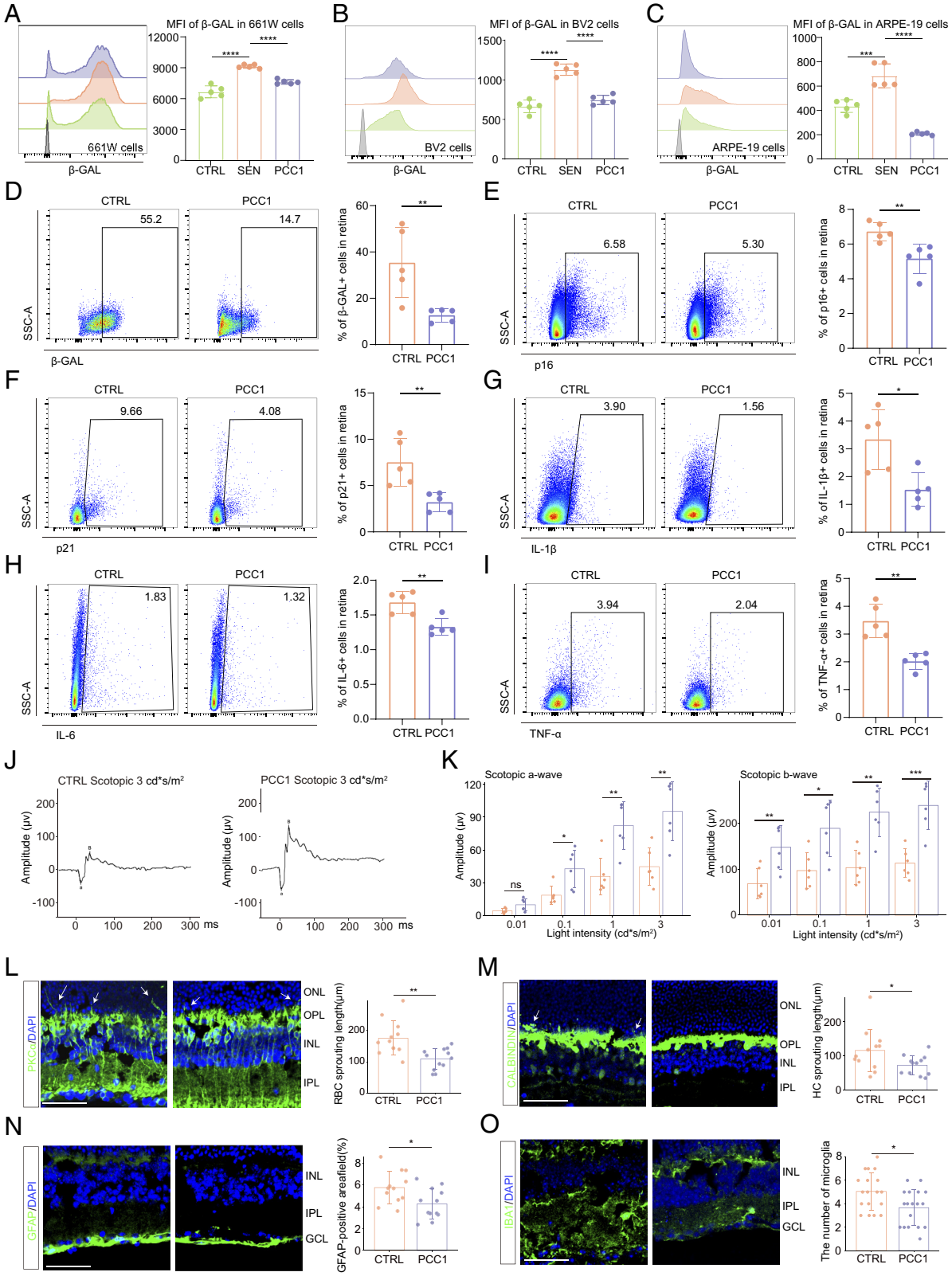


**Fig. 2.** Long-term PCC1 treatment relieved functional and structural impairment in the aged retina by both senolytic and senomorphic effects. (*A–C*) Representative FC histograms (*Left*) and quantification (*Right*) of MFI of β-GAL in 661 W (*A*), BV2 (*B*), and ARPE-19 (*C*) cells among three groups (n = 5/group). (*D–I*) The FC histograms (*Left*) and column charts (*Right*) showing the level of β-GAL (*D*), p16 (*E*), p21 (*F*), IL-6 (*G*), IL-1β (*H*), and TNF-α (*I*) in retinal cells between control and PCC1-treated aged mice (n = 5/group). (*J*) Representative scotopic ERG waveform of aged and PCC1-treated aged mice at a light density of 3 cd*s/m$^2$. (*K*) Bar charts showing the quantification of scotopic ERG amplitudes (n = 6/group). (*L–O*) Representative confocal images of retinal frozen sections of aged (*Upper*) and PCC1-treated (*Middle*) mice and bar charts of quantification (*Right*, n = 6/group). Frozen sections are labeled with PKCα (*L*), Calbindin (*M*), GFAP (*N*), and IBA1 (*O*). Arrows indicate the abnormal sprouting dendrites of RBCs (*L*) and HCs (*M*) which extend beyond OPL into the ONL. (Scale bar, 50 μm.) Data are shown as mean ± SD. *P* values were analyzed using one-way ANOVA with Bonferroni post hoc test (*A–C*) or two-tailed unpaired Student's *t* test (*D–I* and *K–N*) or two-tailed Mann–Whitney *U* test (*O*); ns, nonsignificant, **P* < 0.05, ***P* < 0.01, ****P* < 0.001, and *****P* < 0.0001.

retinal cells obtained from young (6- to 8-wk-old), aged (18- to 20-mo-old), and PCC1-treated aged mice (18- to 20-mo-old). Eleven major cell lineages were determined based on marker genes (Fig. 3*A* and *SI Appendix*, Fig. S3*A*). We then identified differentially expressed genes (DEGs) between aged and young mice (Aged-DEGs), and between PCC1-treated aged mice and aged mice (PCC1-DEGs). Genes down-regulated in Aged-DEGs and then up-regulated in PCC1-DEGs were named up-regulated Rescue-DEGs, while those up-regulated in Aged-DEGs and down-regulated in PCC1-DEGs were named down-regulated Rescue-DEGs (Fig. 3*B*).

To dissect the effects of PCC1 in a cell-type-specific manner, we performed gene ontology (GO) analysis based on the Rescue-DEGs of each subpopulation. The up-regulated Rescue-DEGs were enriched in GO terms associated with neural retinal homeostasis and signaling transmission (Fig. 3*C*), suggesting that PCC1 treatment reversed aging-induced retinal dysfunction. Notably, PCC1 also enhanced mitochondrial function indicated by increased NADH regeneration, an important coenzyme involved in antiaging and antioxidant activity in mitochondria (Fig. 3*C*). Moreover, PCC1 treatment attenuated neural cell death, oxidative stress, and inflammatory MAPK signaling in retinal neurons (Fig. 3*C*).

Furthermore, we utilized the CellChat to analyze the intricate communication networks among different cell types. In terms of cell–cell contact interactions, CADM signaling, which modulates the plasticity of classical excitatory synapses (22), showed a decrease among neurons and glia during aging and remained relatively unchanged after PCC1 treatment (*SI Appendix*, Fig. S3 *B* and *C*). Interestingly, in paracrine interactions, we found that NT signaling, mediated by the Bdnf_Ntrk2 ligand–receptor pair, was down-regulated during aging but rescued by PCC1 (Fig. 3 *D* and *E*). Brain-derived neurotrophic factor (BDNF) is crucial for neuronal survival and has been used to ameliorate cell death in retinal diseases (23). These findings further supported the neuroprotective role of PCC1, highlighting its anti-inflammatory and tissue regenerative properties.

Subsequently, we explored the effects of PCC1 on RPE (Fig. 3*F*). Similarly, the up-regulated Rescue-DEGs in the RPE were enriched in NADH regeneration, cell growth, cell polarity maintenance, and endocytosis. Moreover, PCC1 mitigated biological processes related to inflammation, cell death, and elevated external stress in the RPE. To validate these findings, we further performed RT-qRCR on several Rescue-DEGs with relatively high fold changes in ARPE-19 cells (*SI Appendix*, Fig. S3 *D* and *E*).

Microglia are key mediators of the inflammatory response and pathological disorders in the retina. Single-cell data revealed a higher proportion of microglia in the aged group compared to the young, which was reversed by PCC1 treatment (Fig. 3*G* and *SI Appendix*, Fig. S3*F*). We further validated these findings using FC (Fig. 3*H* and *SI Appendix*, Fig. S3*G*). Furthermore, PCC1 treatment down-regulated several genes related to disease-associated microglia (DAM), including Apoe, Ctsd, Ctsd, Gpnmb, Spp1, Tyrobp, Cd63, and Trem2 (Fig. 3*I*). DAM represents a subset of microglia characterized by up-regulated expression of genes involved in lysosomal, phagocytic, and lipid metabolism pathways compared to their normal counterparts (24, 25). The downregulation of key DAM-related pathological signatures following PCC1 treatment indicated its potential in relieving age-related neurodegenerative transcriptome of microglia.

To conclude, PCC1 reversed age-related dysregulation of genes and rejuvenated various cell types in the retina.

**Clearance of Inferred SnC and Amelioration of SASP Signatures by PCC1 in scRNA-Seq Data.** SenMayo is a novel senescence gene set primarily composed of SASP factors. It demonstrates superior accuracy in identifying SnC in scRNA-seq datasets compared to other existing gene sets (26). Therefore, by applying SenMayo to our sequencing data, we aimed to reveal the transcriptional dynamics of senescent retinal cells following PCC1 treatment. We first compared the cell-type-specific expression of SenMayo features and found that most SenMayo genes were highly expressed in the microglia, VEC, pericytes, macroglia, and RPE (Fig. 4*A*), suggesting their potential susceptibility to cellular senescence and involvement in SASP production. Furthermore, a marked alleviation of the SASP burden was observed in the PCC1 group compared to the aged one (*SI Appendix*, Fig. S4*A*), which was further validated by the RNAscope assay (*SI Appendix*, Fig. S4*B*).

To further dissect the effect of PCC1 at the single-cell level, we identified SnC in scRNA-seq data based on the method of the previous study (26). Simply put, using the SenMayo gene set, we calculated enrichment scores (ES) for each cell in the three groups. SnC were identified as those ranking in the top 10% of ES (Fig. 4*B*, see *Materials and Methods* for details).

We first investigated the functional aspects of this cluster of SnC. Compared to non-SnC, the up-regulated DEGs in SnC were implicated in diverse biological processes (Fig. 4*C*). Notably, NF-κB-mediated signaling, known for governing the inflammatory networks of the SASP secretome (27), was among these GO terms. Wnt, Notch, and HIF-1 signaling may drive and maintain cellular senescence (28–30). Moreover, several pathways are related to the inflammatory response, cytokine production, and cellular response to multiple stimuli, indicating their role in mediating chronic retinal inflammation. Senescent retinal cells also aggressively participate in remodeling local microenvironments, including angiogenesis and extracellular matrix reorganization, potentially through secreting VEGF and its proteases (11).

We then used t-SNE plots to visualize the distribution of SnC across the three groups (Fig. 4*D* and *SI Appendix*, Fig. S4*C*), which showed that SnC accumulated in the aged retina and this increase was substantially reversed after PCC1 treatment (*SI Appendix*, Table S1), further underscoring the effectiveness of PCC1 in eliminating SnC. When analyzing the source of SnC, we found that they were predominantly composed of non-neurons including RPE, microglia, VEC, pericytes, and macroglia (Fig. 4*E*). To further validate this, we colabeled β-GAL with commercially available FC antibodies targeting specific surface markers for retinal cells. CD11B targets microglia, CD73 is expressed in mature rod photoreceptor (31) and CD90.2 (Thy1.2) targets mainly ganglion cells plus a small population of amacrine cells (32). FC suggested that microglia exhibited the highest expression of β-gal, followed by CD90.2 + cells and rods (Fig. 4*F*), which was in line with single-cell predictions (Fig. 4*E*). The β-gal activity in these cell clusters across the three groups (*SI Appendix*, Fig. S4*D*) also corresponded to the expression trend in the whole retina.

We further investigated the molecular basis underlying the senolytic and senomorphic role of PCC1. The up-regulated PCC1-DEGs in SnC were enriched in pathways related to apoptosis signaling, programmed cell death, and the cellular response to increased ROS in several cell types, particularly RPE and microglia (Fig. 4*G*), which aligned with the senolytic mechanism previously reported (20). Moreover, among the up-regulated pathways in SnC, p38MAPK has also been identified as a critical SASP regulator (33) aside from NF-κB signaling. We calculated gene set scores for these two pathways in SnC from the two groups and found that PCC1 elicited an inhibitory effect on these SASP

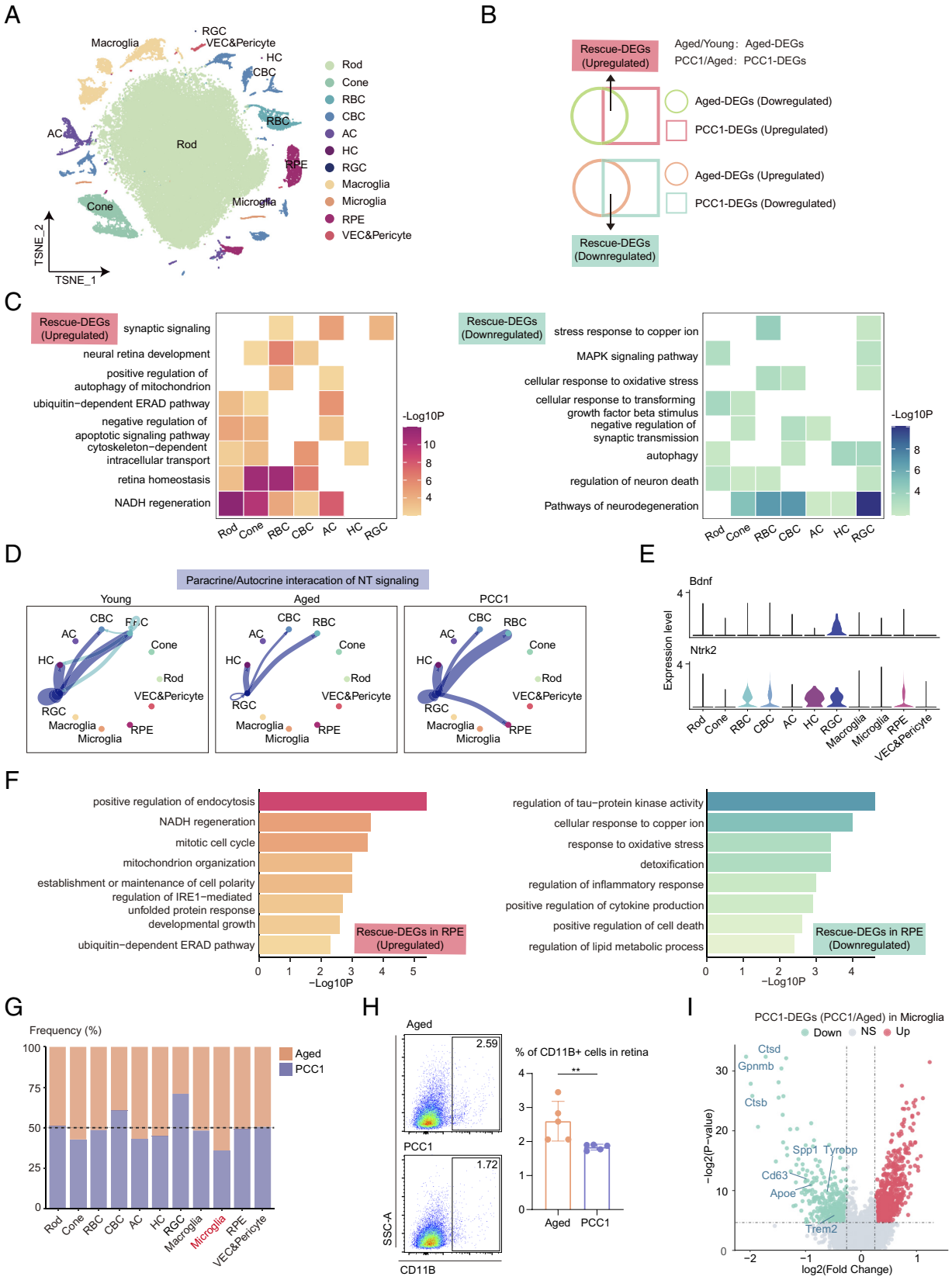


**Fig. 3.** The seotherapeutic effects of PCC1 treatment on the aged retina evaluated by single-cell analysis. (*A*) t-SNE plot showing the distribution of different retinal cell types. (*B*) Venn diagrams showing the Aged-DEGs, PCC1-DEGs, and Rescue-DEGs. (*C*) Heatmaps showing GO terms enriched for the up-regulated (*Left*) and down-regulated (*Right*) Rescue-DEGs of different neuronal cell types after PCC1 treatment. (*D*) Circle plots showing the inferred NT signaling networks among three groups. Edge width represents the communication probability. (*E*) Violin plots showing the expression of the ligand–receptor involved in the inferred NT signaling pathway. (*F*) Bar plots showing the GO terms enriched for the up-regulated (*Left*) and down-regulated (*Right*) Rescue-DEGs of RPE after PCC1 treatment. (*G*) Bar plot showing the ratios of different retinal cell types of PCC1-treated mice compared to aged mice derived from scRNA-seq data. (*H*) Representative flow charts (*Left*) and quantification (*Right*) of the proportion of microglia from the retina of control and PCC1 group (n = 5/group). Data are shown as mean ± SD and were analyzed using unpaired two-tailed Student's *t* test; $^{**}P < 0.01$. (*I*) Volcano plot showing up-regulated and down-regulated PCC1-DEGs of microglia.

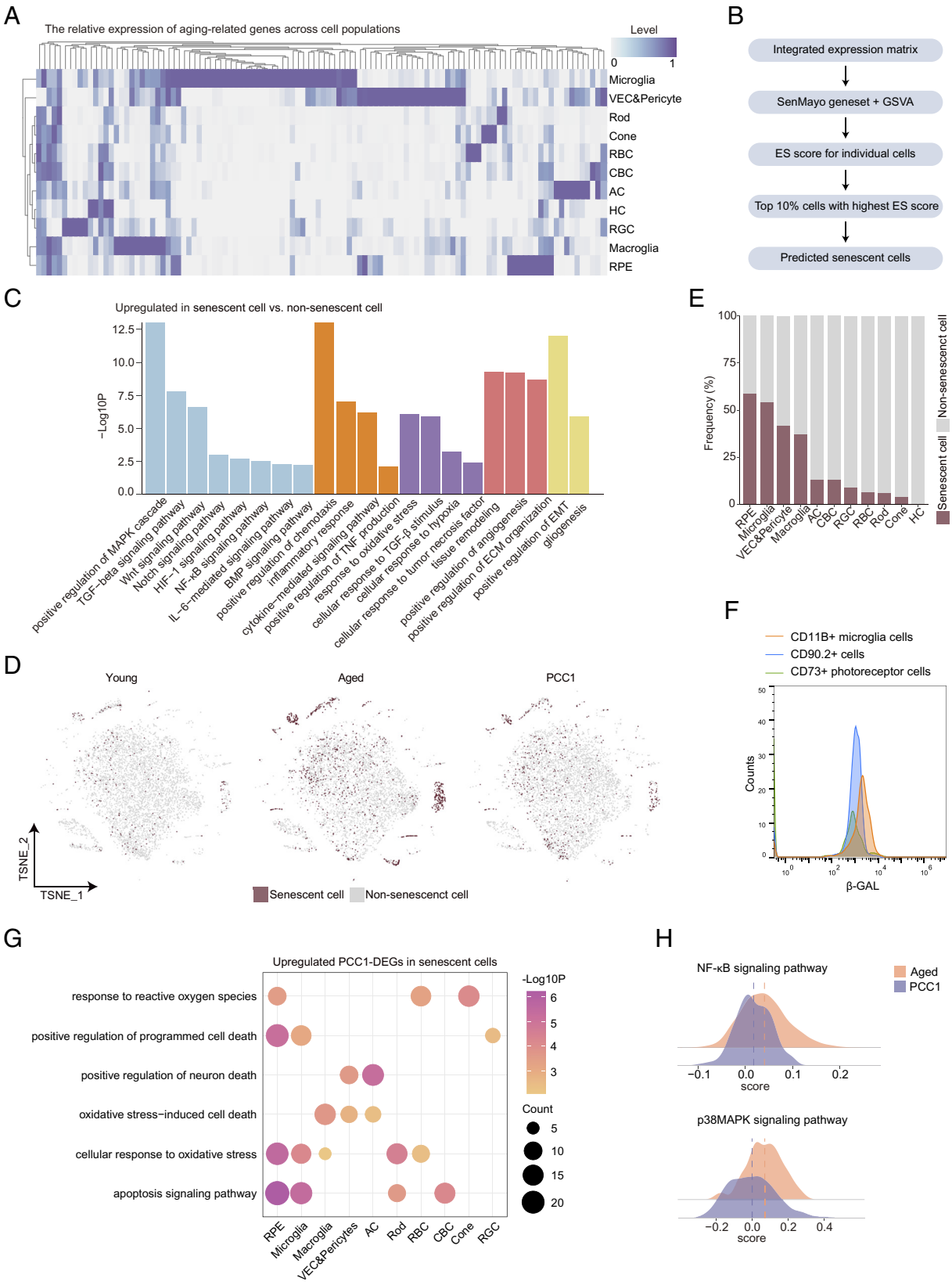


**Fig. 4.** Clearance of inferred SnC and amelioration of SASP signatures by PCC1 in scRNA-seq data. (*A*) Heatmap showing the expression pattern of SASP-related genes in different cell types in the retina. (*B*) Schematic diagram showing predication of SnC in scRNA-seq data. (*C*) Bar plots showing the GO terms enriched for the up-regulated DEGs of SnC compared to non-SnC in the retina. Similar GO terms are placed together in the same color. (*D*) t-SNE plots showing the distribution of SnC in the retina of three groups. (*E*) Bar plot showing the percentage of SnC in all retinal cells of three groups. (*F*) FC overlay histogram showing the expression of β-gal of CD11B+ microglia cells (orange), CD90.2+ cells (blue), and CD73+ rods (green). Fluorescence intensity is represented on the x-axis and count of the events on the y-axis. (*G*) Dot plot showing pathways enriched for the up-regulated PCC1-DEGs in SnC of different retinal cell types from the retina. The color key indicates the *P* value. The dot size is proportional to the number of genes enriched in indicated pathways. (*H*) Ridge plots showing the gene set scores of NF-κB and p38MAPK signaling pathways of SnC from the aged and PCC1 groups.

modulators (Fig. 4*H*), suggesting that PCC1 might act as a senomorphic at least by targeting NF-κB and p38MAPK signaling.

**In Vivo and In Vitro Experimental Validation of the Senolytic Effect by PCC1.** As uncovered by bioinformatic analysis that cell death was enriched in SnC from the PCC1 group across various cell types, we aimed to provide direct evidence of senolysis induced by PCC1. We first identified apoptotic cells in situ via the TUNEL assay which exhibited a substantial increase in apoptosis activity after PCC1 treatment (Fig. 5*A*). Remarkably, the RPE layer showed a relatively high ratio of apoptotic cells indicating that RPE could be a great source of SnC, which was consistent with our single-cell prediction (Fig. 4*E*).

We then investigated the in vitro effect of PCC1. The CCK-8 assay revealed that PCC1 had no significant impact on the viability of control cells at concentrations up to 200 μM. While for SnC, PCC1 demonstrated cytotoxicity starting at 50 μM and its senolytic effect became more pronounced as the concentration increased across all three cell lines (Fig. 5*B* and *SI Appendix*, Fig. S5 *A* and *B*), which aligned with previous reports that PCC1 is a broad-spectrum senolytic (20). Moreover, we performed annexin V and propidium iodide (PI) staining on multiple retinal cell lines for the quantifiable apoptosis assay using FC (Fig. 5*C* and *SI Appendix*, Fig. S5 *C* and *D*), which supported cell viability experiments.

**PCC1 Treatment Ameliorated Age-Related Chronic Inflammation Both Locally and Systemically.** Aging is characterized by systemic chronic inflammation (SCI), a state of persistent and low-grade inflammation in various tissues and organs, which ultimately causes cumulative systemic damage including organ dysfunction and age-related pathologies. The SCI state in older individuals is thought to be driven largely by cellular senescence and SASP (34). In such context, we next explored the effects of systemic administration of PCC1 on systemic and retinal inflammation.

We measured the plasma levels of proinflammatory molecules such as IL-6, IL-1β, and TNF-α by the enzyme-linked immunosorbent assay. As shown in Fig. 5*D*, these cytokines were significantly elevated in the aged circulation but exhibited a general decrease following long-term PCC1 treatment. In addition to reduction of several inflammatory factors in the whole retina by PCC1 (Fig. 2 *G–I* and *SI Appendix*, Fig. S2*K*), we further calculated the SASP gene set score for each cell type in the aged and PCC1 group using single-cell data. Among them, microglia, the predominant inflammation mediator in the retina, displayed the most notable suppression of SASP features (*SI Appendix*, Fig. S5 *E* and *F*). Moreover, FC of retinal samples (Fig. 5 *E–G*) and the BV2 cell line (*SI Appendix*, Fig. S5 *G–I*) validated that PCC1 mitigated the inflammatory phenotype of microglia induced by aging.

Altogether, long-term PCC1 treatment alleviated age-related chronic inflammation both locally and systemically.

**The Therapeutic Potential of PCC1 As a Senolytic and Senomorphic Agent in Treating Age-Related Retinal Disorders.** As cellular senescence exerts a deleterious effect during retinal aging, we explored whether it is implicated in age-related retinal disorders by analyzing two published scRNA-seq datasets derived from choroid and RPE tissue of patients with neovascular AMD (nAMD) (35) and retinal tissue from a mouse model of experimental DR (36), respectively.

We first investigated the nAMD data (GSE135922) and clustered the cells into 11 populations as the original study did (Fig. 6*A* and *SI Appendix*, Fig. S4*A*). We then assessed the SenMayo signatures of these cells from both normal and diseased groups, with the latter showing higher score (Fig. 6*B*). To further elucidate the role of SnC in nAMD progression, we identified SnC as previously described and found that they were primarily composed of fibroblasts and were notably increased in patients with nAMD compared to healthy controls (*SI Appendix*, Fig. S4 *B–D*).

Next, we employed CellChat to characterize how SnC influence their neighbors and orchestrate the signaling network involved in age-related disorders. Globally, SnC exhibited a relatively high communication strength and engaged in numerous interactions with other cell types, both as senders and receivers (Fig. 6 *C* and *D* and *SI Appendix*, Fig. S6*E*). Focusing on SnC as the source, we depicted the inferred signaling pathways exerted on endothelial cells and pericytes (*SI Appendix*, Fig. S6*F*), both of which play key roles in choroidal neovascularization in nAMD. SnC participated in diverse pathways with these cell types, many of which have been associated with pathological angiogenesis and local inflammation. For example, SnC unexpectedly exhibited high expression of ligands VEGF and ANGPTL4, which engages in vascular permeability regulation and angiogenesis (37, 38) (*SI Appendix*, Fig. S6 *G* and *H*). Moreover, JAG1 was also up-regulated in SnC, a ligand known to activate the NOTCH signaling pathway and promote neovascularization while the expression of DLL4, another ligand with contrasting effects (39), was not increased (*SI Appendix*, Fig. S7*A*). Additionally, SnC were involved in the IL-6 signaling pathway (*SI Appendix*, Fig. S7*B*), which has dual proinflammatory and proangiogenic effects in nAMD.

We then analyzed the DR dataset (GSE178121), which included samples from normal and STZ-induced diabetic retina. The cells were annotated into 10 clusters (Fig. 6*E* and *SI Appendix*, Fig. S7*C*) and the SASP burden was up-regulated in neurons (rods, cones, RBCs), Microglia, and VEC in the DR group (Fig. 6*F*). SnC were predominantly derived from microglia, VEC, and RPE, with a notable increase in the DR group (Fig. 6 *G* and *H* and *SI Appendix*, Fig. S7 *D* and *E*). Next, we focused on the biological functions of SnC in DR and found that up-regulated DEGs in SnC were enriched in angiogenesis, epithelial cell migration, growth factor pathways, and neuroinflammatory responses (Fig. 6*I*), suggesting that SnC may exacerbate DR by mediating pathological responses. We further interrogated intercellular communication between SnC and other cells using CellChat. SnC were identified as the primary source for the MIF, PSAP, PTN, and TGFb signaling pathways (*SI Appendix*, Fig. S7 *F–I*). These signalings have been implicated in the migration and proliferation of endothelial cells (40, 41) and promote angiogenesis in DR. These proangiogenic signaling pathways induced by SnC further highlighted their potential role in choroidal neovascularization during DR progression.

To further verify the therapeutic effect of PCC1 on DR via senolysis, we exposed human retinal microvascular endothelial cells (HRMEC) to high concentrations of glucose to establish the in vitro DR model. FC analysis revealed an increase in cellular senescence in the DR model which was subsequently reduced after PCC1 treatment (Fig. 6 *J–L*). Furthermore, PCC1 remarkably reduced the secretion of IL-6 and VEGF-A (Fig. 6 *M–O*), indicating its ability to mitigate the proinflammatory and proangiogenic properties of glucose-induced HRMEC.

Overall, SnC contributed to pathological responses in age-related retinal disorders, and PCC1 displayed great promise in slowing the progression of these diseases.

## Discussion

This study revealed a significant elevation in cellular senescence burden during aging, accompanied by a comprehensive decline in visual function and retinal structure. Long-term PCC1

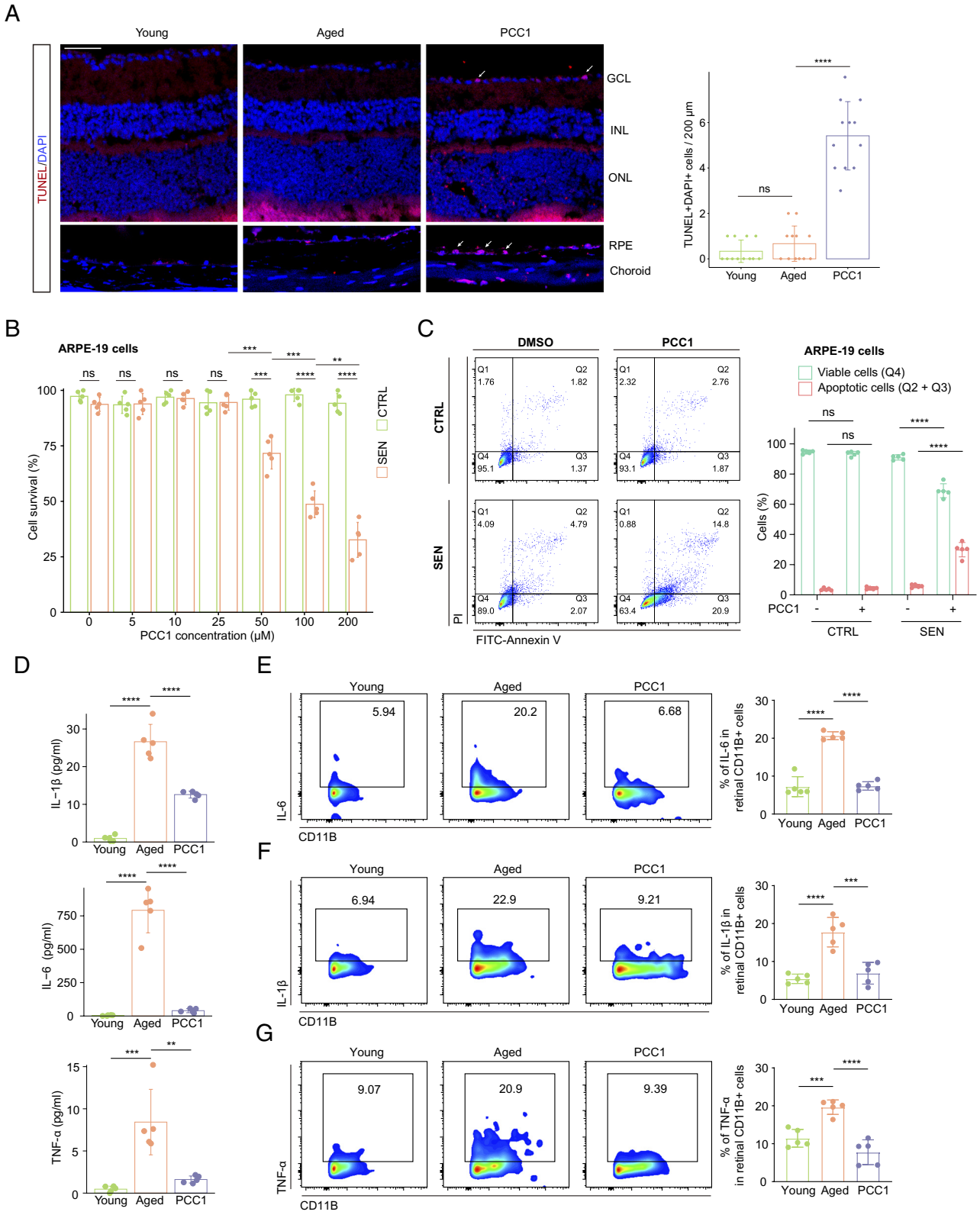


**Fig. 5.** PCC1 demonstrated senolytic and senomorphic effects both in vivo and in vitro. (*A*) Representative confocal images of retinal frozen sections stained with the TUNEL assay among three groups and bar charts of quantification (n = 6/group). Arrows indicate the representative apoptotic cells. (Scale bar, 50 μm.) (*B*) Bar plot showing the CCK-8 assay on control and SnC of ARPE-19 cell line upon treatment of PCC1 (n = 5/group). (*C*) Representative flow charts (*Left*) and quantification (*Right*) of the annexin V/PI apoptotic assay on control and SnC of ARPE-19 cell line upon treatment of PCC1 (n = 5/group). (*D*) The plasma levels of IL-6, IL-1β, and TNF-α in different groups were measured by the ELISA assay (n = 5/group). (*E*–*G*) The FC histograms (*Left*) and column charts (*Right*) showing the level of IL-6 (*E*), IL-1β (*F*), and TNF-α (*G*) in retinal microglia among three groups (n = 5/group). Data are shown as mean ± SD. *P* values were analyzed using the Kruskal–Wallis test with Bonferroni post hoc test (*A*) or two-tailed unpaired Student's *t* test (*B* and *C*) or one-way ANOVA with Bonferroni post hoc test (*D*–*G*); ns, nonsignificant, **P* < 0.05, ***P* < 0.01, ****P* < 0.001, and *****P* < 0.0001.

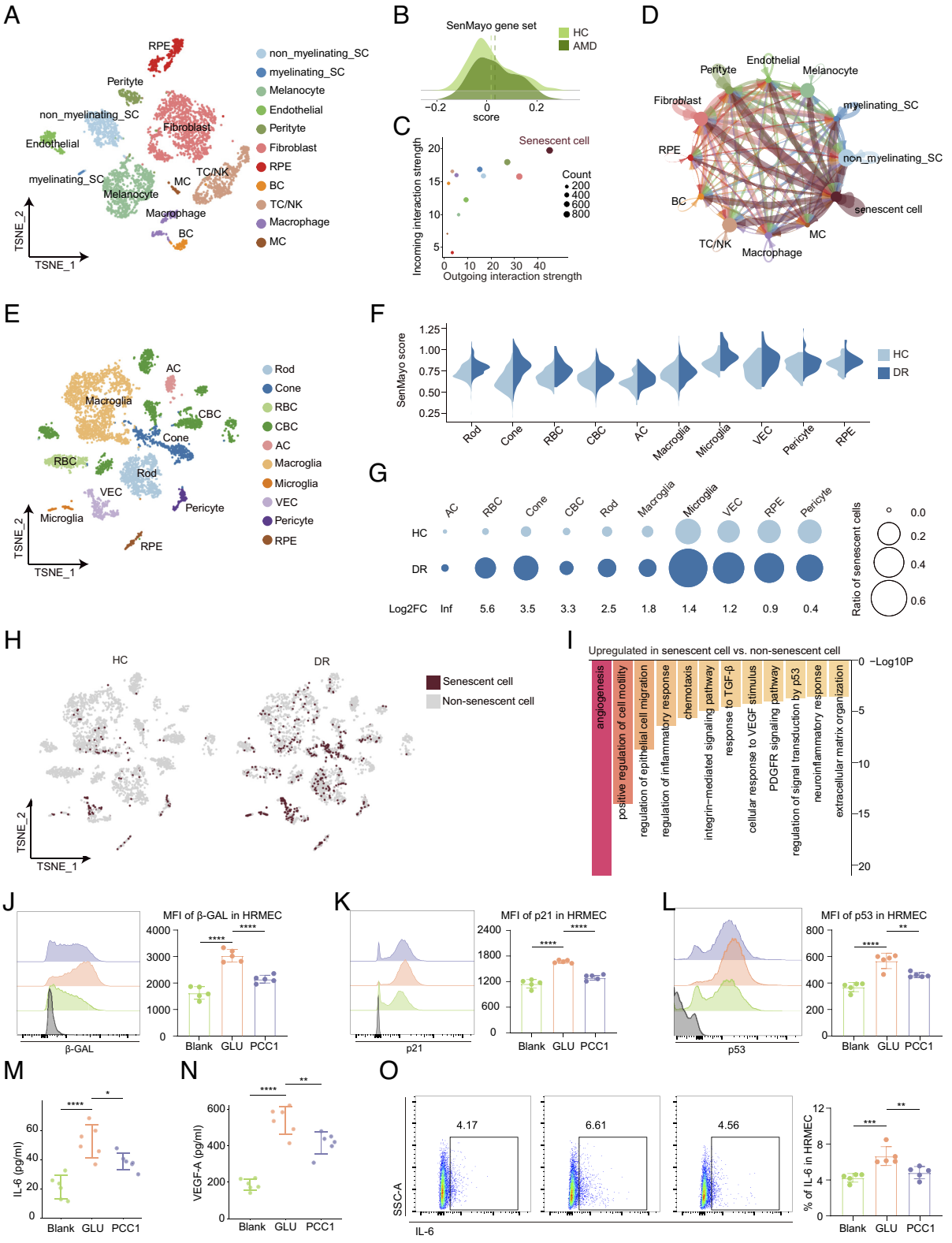


**Fig. 6.** The therapeutic potential of PCC1 as a senolytic and senomorphic agent in treating age-related retinal disorders. (*A*) t-SNE plot showing the distribution of different RPE and choroidal cell types. (*B*) Ridge plot showing the expression of SASP signatures from normal and AMD groups. The dashed lines indicate the mean values. (*C*) Dot plot showing the incoming and outgoing interaction pattern of different cell types in the cell–cell communication. (*D*) Network visualization showing cell–cell interactions among different cell types. The line color indicates the source cell types. The edge width indicates the relative interaction strength between a given cell pair, and the dot size indicates the number of cells in each cell type. (*E*) t-SNE plot showing the distribution of different retinal cell types. (*F*) Split violin plots showing the ES of SASP-related genes across different cell types between the two groups. (*G*) Bubble plots showing the changes in cell ratios of SnC in the retina between the two groups. The numbers at the bottom indicate the log2FC values of the cell ratios (DR/Normal). The size of the dots represents the ratios of cells. (*H*) t-SNE plot showing the distribution of SnC in the retina between the two groups. (*I*) Bar plot showing the GO terms enriched for the up-regulated DEGs of SnC compared to non-SnC. (*J*–*L*) Representative FC histogram (*Left*) and quantification (*Right*) of MFI of β-GAL (*J*), p21 (*K*), and p53 (*L*) of HRMEC from different groups (n = 5/group). (*M* and *N*) The supernatant level of IL-6 and VEGF-A in different groups was measured by ELISA (n = 6/group). (*O*) Representative flow charts (*Left*) and quantification (*Right*) of the proportion of IL-6 in HRMEC from different groups (n = 5/group). Data are shown as mean ± SD, and *P* values were analyzed using one-way ANOVA with Bonferroni post hoc test (*J*–*O*); **P* < 0.05, ***P* < 0.01, ****P* < 0.001, and *****P* < 0.0001.

treatment successfully reduced the accumulation of SnC and secretion of SASP, resulting in functional and morphological rejuvenation of the degenerative aging process in the retina. Using a high-throughput sequencing tool, we constructed a detailed transcriptome atlas of PCC1-treated retina, uncovering the molecular mechanisms of PCC1 as a senolytic and senomorphic. PCC1 exerted neuroprotective and anti-inflammatory effects that reverse retinal aging. By further mining the scRNA-seq databases of nAMD and DR, we investigated the senescence burden and its implications in age-related retinal diseases and confirmed the therapeutic potential of PCC1 in these disorders in vitro.

Cellular senescence is the fundamental driver of aging and age-related diseases. Although senescence refers to a permanent cell cycle arrest, postmitotic retinal cells undergo age-related stressors similar to those of proliferating cells, generating senescence-like signatures (42). Stress-induced senescence also occurs in terminally differentiated cells such as neurons (43) and adipocytes (44). This state is likely triggered by oxidative stress regulation and the response to DNA damage (45).

The senolytic activity of PCC1 lies in its selective proapoptotic properties in SnC, which is mediated by modulating the expression pattern of the BCL-2 superfamily and aggravating mitochondrial dysfunction during cellular senescence (20). The upregulation of the apoptotic signaling pathway and the response to oxidative stress by PCC1 were substantiated by our data. Compared to other canonical senolytics including dasatinib, quercetin, and ABT-263, which have reported side effects and low oral availability, PCC1, as a natural compound, stands out for its promising safety and in vivo efficacy profile. Apart from indirect reduction of SASP through senolysis, PCC1 directly suppresses those inflammatory mediators by blocking the upstream signaling which greatly potentiates the senotherapeutic effect of PCC1 in comparison to other senolytics.

Although the molecular weight of PCC1 (866.77) exceeds the limits of the BRB, PCC1 indeed permeated the blood-retinal barrier (BRB) and exerted in situ senolytic effect, which could be explained by defects in both inner and outer BRB in aged rodent retina. Remarkable breakdown of inner BRB indicated by tracer horseradish peroxidase (molecular weight: 44,000) and decreased occludin expression, was detected (46). An irregular pattern of tight junction of RPE was also reported in aged mice, including splitting, separation, and fragmentation of the cytoskeleton (47). Additionally, PCC1 likely rejuvenates the retina indirectly by modulating the systemic inflammatory status.

The rejuvenating capacity of PCC1 in the aged retina has expanded its therapeutic effects in age-related retinal diseases. To mimic DR in vitro, we induced senescence in HRMEC and confirmed the efficacy of PCC1 in reducing senescence burden. Multiple lines of evidence also supported the detrimental role of cellular senescence in age-related retinopathy and elimination of senescence burden contributed to the alleviation of these disorders, which has been validated in cell models, animal models, and patients with AMD (48, 49), diabetic retinopathy (42, 50, 51), and glaucoma (52–54). These findings further provided the basis for expanding the therapeutic potential PCC1 in the treatment of senescence-related retinopathy.

In summary, we delineated the distinct cell compositions and phenotypes during natural retinal aging as well as confirmed the rejuvenating effect of PCC1 on the aged retina. Through the selective depletion of SnC and inhibition of the SASP, PCC1 reversed the structural and functional impairment in the aging retina. These findings position PCC1 as a promising candidate for the treatment of age-related retinal diseases. Our study offers an in-depth view of the phytochemical compound in retinal diseases based on its safety and efficacy profile, paving the way for future clinical research in this field.

## Materials and Methods

**Animals, Drug Treatment, and Experiments.** The mice were divided into three groups: 1) Young mice (6 to 8 wk) received standard diet; 2) aged mice (14 to 16 mo) received standard diet; and 3) the PCC1 group with aged mice (14 to 16 mo) received tailor-made diet. PCC1 was mixed with the regular chow with a concentration of 8 mg/kg. The administration of PCC1 lasted for 4 mo. Before the mice were killed, the mice were subjected to ERG measurement. Retinal tissue was then harvested for UPLC, IF, RNAscope, qPCR, and FC analysis. Detailed descriptions are provided in *SI Appendix*.

**Cell Culture and Treatment Protocols.** 661 W, APRE-19, BV2, and human retinal microvascular endothelial cell cell lines were used for in vitro experiments. The cells were subjected to senescence induction, establishment of the in vitro DR model, and cell viability assay. Detailed descriptions are provided in *SI Appendix*.

**scRNA-Seq Analysis.** The scRNA-seq data are deposited in the Genome Sequence Archive in BIG Data Center, Beijing Institute of Genomics under GSA Accession No. CRA011488. Detailed bioinformatic analysis is provided in *SI Appendix*.

**Data, Materials, and Software Availability.** Single-cell RNA sequencing data have been deposited in Genome Sequence Archive in BIG Data Center, Beijing Institute of Genomics (CRA011488) (55).

**ACKNOWLEDGMENTS.** This research was funded by the National Key R&D Project of China (2020YFA0112701); the National Natural Science Foundation of China (82171057); and Science and Technology Program of Guangzhou, China (202206080005).

Author affiliations: [a]State Key Laboratory of Ophthalmology, Zhongshan Ophthalmic Center, Sun Yat-sen University, Guangdong Provincial Key Laboratory of Ophthalmology and Visual Science, Guangzhou 510060, People's Republic of China; and [b]Department of Clinical Medicine, Zhongshan School of Medicine, Sun Yat-sen University, Guangzhou 510060, People's Republic of China

1. D. J. Baker, R. C. Petersen, Cellular senescence in brain aging and neurodegenerative diseases: Evidence and perspectives. *J. Clin. Invest.* **128**, 1208–1216 (2018).
2. L. Huang *et al.*, Deep Sc-RNA sequencing decoding the molecular dynamic architecture of the human retina. *Sci. China Life Sci.* **66**, 496–515 (2023).
3. R. Li, Y. Liang, B. Lin, Accumulation of systematic TPM1 mediates inflammation and neuronal remodeling by phosphorylating PKA and regulating the FABP5/NF-κB signaling pathway in the retina of aged mice. *Aging Cell* **21**, e13566 (2022).
4. S. Ferdous *et al.*, Age-related retinal changes in wild-type C57BL/6J mice between 2 and 32 months. *Invest. Ophthalmol. Vis. Sci.* **62**, 9 (2021).
5. M. A. Samuel *et al.*, LKB1 and AMPK regulate synaptic remodeling in old age. *Nat. Neurosci.* **17**, 1190–1197 (2014).
6. S. R. Flaxman *et al.*, Global causes of blindness and distance vision impairment 1990–2020: A systematic review and meta-analysis. *Lancet Global Health* **5**, e1221–e1234 (2017).
7. D. Muñoz-Espín, M. Serrano, Cellular senescence: From physiology to pathology. *Nat. Rev. Mol. Cell Biol.* **15**, 482–496 (2014).
8. F. Rodier, J. Campisi, Four faces of cellular senescence. *J. Cell Biol.* **192**, 547–556 (2011).
9. J. Blasiak, Senescence in the pathogenesis of age-related macular degeneration. *Cell Mol. Life Sci.* **77**, 789–805 (2020).
10. G. Nelson *et al.*, A senescent cell bystander effect: Senescence-induced senescence. *Aging Cell* **11**, 345–349 (2012).
11. S. Chaib, T. Tchkonia, J. L. Kirkland, Cellular senescence and senolytics: The path to the clinic. *Nat. Med.* **28**, 1556–1568 (2022).
12. R. J. Pignolo, J. F. Passos, S. Khosla, T. Tchkonia, J. L. Kirkland, Reducing senescent cell burden in aging and disease. *Trends Mol. Med.* **26**, 630–638 (2020).
13. W. Huang, L. J. Hickson, A. Eirin, J. L. Kirkland, L. O. Lerman, Cellular senescence: The good, the bad and the unknown. *Nat. Rev. Nephrol.* **18**, 611–627 (2022).
14. C. Aguayo-Mazzucato *et al.*, Acceleration of β cell aging determines diabetes and senolysis improves disease outcomes. *Cell Metabolism* **30**, 129–142.e4 (2019).
15. M. Xu *et al.*, Senolytics improve physical function and increase lifespan in old age. *Nat. Med.* **24**, 1246–1256 (2018).
16. US National Library of Medicine, Safety and Tolerability Study of UBX1325 in Patients With Diabetic Macular Edema or Neovascular Age-Related Macular Degeneration. Identifier NCT04537884. https://classic.clinicaltrials.gov/ct2/show/results/NCT04537884. Accessed 12 May 2023.
17. US National Library of Medicine, Safety, Tolerability and Evidence of Activity Study of UBX1325 in Patients With Diabetic Macular Edema (BEHOLD). Identifier NCT04857996. https://classic.clinicaltrials.gov/ct2/show/NCT04857996. Accessed 12 May 2023.

18. J. Chen *et al.*, Relationship between neuroprotective effects and structure of procyanidins. *Molecules* **27**, 2308 (2022).
19. L. L. Koteswari, S. Kumari, A. B. Kumar, R. R. Malla, A comparative anticancer study on procyanidin C1 against receptor positive and receptor negative breast cancer. *Nat. Prod. Res.* **34**, 3267–3274 (2020).
20. Q. Xu *et al.*, The flavonoid procyanidin C1 has senotherapeutic activity and increases lifespan in mice. *Nat. Metab.* **3**, 1706–1726 (2021).
21. D. Grün, A. van Oudenaarden, Design and analysis of single-cell sequencing experiments. *Cell* **163**, 799–810 (2015).
22. A. Ribic, X. Liu, M. C. Crair, T. Biederer, Structural organization and function of mouse photoreceptor ribbon synapses involve the immunoglobulin protein synaptic cell adhesion molecule 1. *J. Comp. Neurol.* **522**, 900–920 (2014).
23. K. Ikeda *et al.*, BDNF attenuates retinal cell death caused by chemically induced hypoxia in rats. *Invest. Ophthalmol. Vis. Sci.* **40**, 2130–2140 (1999).
24. A. Deczkowska *et al.*, Disease-associated microglia: A universal immune sensor of neurodegeneration. *Cell* **173**, 1073–1081 (2018).
25. H. Keren-Shaul *et al.*, A unique microglia type associated with restricting development of Alzheimer's disease. *Cell* **169**, 1276–1290.e17 (2017).
26. D. Saul *et al.*, A new gene set identifies senescent cells and predicts senescence-associated pathways across tissues. *Nat. Commun.* **13**, 4827 (2022).
27. J. C. Acosta *et al.*, A complex secretory program orchestrated by the inflammasome controls paracrine senescence. *Nat. Cell Biol.* **15**, 978–990 (2013).
28. W. Gong *et al.*, Brahma-related gene-1 promotes tubular senescence and renal fibrosis through Wnt/β-catenin/autophagy axis. *Clin. Sci. (Lond)* **135**, 1873–1895 (2021).
29. Y. V. Teo *et al.*, Notch signaling mediates secondary senescence. *Cell Rep.* **27**, 997–1007.e5 (2019).
30. J. Liu *et al.*, Demethyleneberberine induces cell cycle arrest and cellular senescence of NSCLC cells via c-Myc/HIF-1α pathway. *Phytomedicine* **91**, 153678 (2021).
31. H. Koso *et al.*, CD73, a novel cell surface antigen that characterizes retinal photoreceptor precursor cells. *Invest. Ophthalmol. Vis. Sci.* **50**, 5411–5418 (2009).
32. I. D. Raymond, A. Vila, U.-C.N. Huynh, N. C. Brecha, Cyan fluorescent protein expression in ganglion and amacrine cells in a thy1-CFP transgenic mouse retina. *Mol. Vis.* **14**, 1559–1574 (2008).
33. A. Freund, C. K. Patil, J. Campisi, p38MAPK is a novel DNA damage response-independent regulator of the senescence-associated secretory phenotype. *EMBO J.* **30**, 1536–1548 (2011).
34. D. Furman *et al.*, Chronic inflammation in the etiology of disease across the life span. *Nat. Med.* **25**, 1822–1832 (2019).
35. A. P. Voigt *et al.*, Single-cell transcriptomics of the human retinal pigment epithelium and choroid in health and macular degeneration. *Proc. Natl. Acad. Sci. U.S.A.* **116**, 24100–24107 (2019).
36. L. Sun *et al.*, Single cell RNA sequencing (scRNA-Seq) deciphering pathological alterations in streptozotocin-induced diabetic retinas. *Exp. Eye Res.* **210**, 108718 (2021).
37. X. Yang, Y. Cheng, G. Su, A review of the multifunctionality of angiopoietin-like 4 in eye disease. *Biosci. Rep.* **38**, BSR20180557 (2018).
38. S. Babapoor-Farrokhran *et al.*, Angiopoietin-like 4 is a potent angiogenic factor and a novel therapeutic target for patients with proliferative diabetic retinopathy. *Proc. Natl. Acad. Sci. U.S.A.* **112**, E3030–E3039 (2015).
39. R. Benedito *et al.*, The notch ligands Dll4 and Jagged1 have opposing effects on angiogenesis. *Cell* **137**, 1124–1135 (2009).
40. A. M. Abu El-Asrar *et al.*, The proinflammatory and proangiogenic macrophage migration inhibitory factor is a potential regulator in proliferative diabetic retinopathy. *Front Immunol.* **10**, 2752 (2019).
41. X. Zhu *et al.*, The effects of pleiotrophin in proliferative diabetic retinopathy. *PLoS One* **10**, e0115523 (2015).
42. M. Oubaha *et al.*, Senescence-associated secretory phenotype contributes to pathological angiogenesis in retinopathy. *Sci. Transl. Med.* **8**, 362ra144 (2016).
43. J. R. Herdy *et al.*, Increased post-mitotic senescence in aged human neurons is a pathological feature of Alzheimer's disease. *Cell Stem Cell* **29**, 1637–1652.e6 (2022).
44. T. Minamino *et al.*, A crucial role for adipose tissue p53 in the regulation of insulin resistance. *Nat. Med.* **15**, 1082–1087 (2009).
45. Y. Okuno, A. Nakamura-Ishizu, K. Otsu, T. Suda, Y. Kubota, Pathological neoangiogenesis depends on oxidative stress regulation by ATM. *Nat. Med.* **18**, 1208–1216 (2012).
46. T. Chan-Ling *et al.*, Inflammation and breakdown of the blood-retinal barrier during "Physiological Aging" in the rat retina: A model for CNS aging. *Microcirculation* **14**, 63–76 (2007).
47. J. Y. W. Ma *et al.*, Aging induces cell loss and a decline in phagosome processing in the mouse retinal pigment epithelium. *Neurobiol. Aging* **128**, 1–16 (2023).
48. J.-B. Chae *et al.*, Targeting senescent retinal pigment epithelial cells facilitates retinal regeneration in mouse models of age-related macular degeneration. *GeroScience* **43**, 2809–2833 (2021).
49. F. Gao *et al.*, Elimination of senescent cells inhibits epithelial-mesenchymal transition of retinal pigment epithelial cells. *Exp. Eye Res.* **223**, 109207 (2022).
50. S. Crespo-Garcia *et al.*, Pathological angiogenesis in retinopathy engages cellular senescence and is amenable to therapeutic elimination via BCL-xL inhibition. *Cell Metab.* **33**, 818–832.e7 (2021).
51. M. López-Luppo *et al.*, Cellular senescence is associated with human retinal microaneurysm formation during aging. *Invest. Ophthalmol. Vis. Sci.* **58**, 2832 (2017).
52. Q. Xu *et al.*, Stress induced aging in mouse eye. *Aging Cell* **21**, e13737 (2022).
53. D. Skowronska-Krawczyk *et al.*, p16INK4a upregulation mediated by SIX6 defines retinal ganglion cell pathogenesis in glaucoma. *Mol. Cell* **59**, 931–940 (2015).
54. L. R. Rocha *et al.*, Early removal of senescent cells protects retinal ganglion cells loss in experimental ocular hypertension. *Aging Cell* **19**, e13089 (2020).
55. Y. Liu *et al.*, Senolytic and senomorphic agent PCC1 alleviates structural and functional decline in aged retina. Genome Sequence Archive. https://ngdc.cncb.ac.cn/gsa/browse/CRA011488. Deposited 19 June 2023.